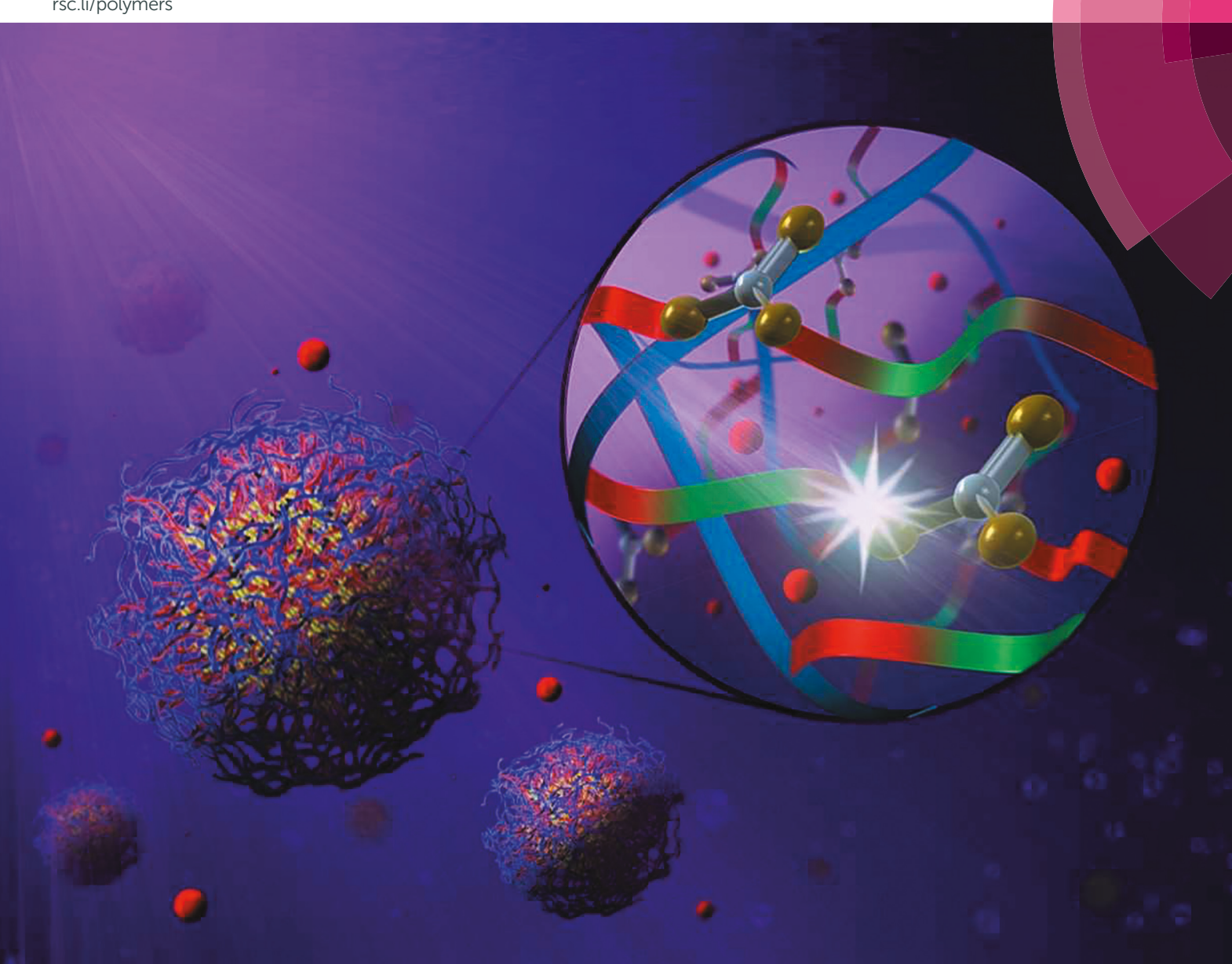
Polymer Chemistry

rsc.li/polymers



ISSN 1759-9962



PAPER

Polymer Chemistry



PAPER View Article Online
View Journal | View Issue



Cite this: *Polym. Chem.*, 2019, **10**, 3841

Nanonetwork photogrowth expansion: Tailoring nanoparticle networks' chemical structure and local topology†

Michael W. Lampley, a,b Enkhjargal Tsogtgerela and Eva Harth **D***

The manipulation of covalent polymer networks in the bulk or in the nanoscale seeks to broaden material property variations from an existing parent structure with the possibility to make fundamental changes in nanoparticle compositions which is otherwise difficult to accomplish through bottom up approaches. In this contribution, a parent nanoparticle network prepared by an intermolecular chain cross-linking process containing trithiocarbonate photoactive cross-linking groups has been investigated in its ability to form various novel nanonetworks through a photogrowth expansion process using 10-phenylphenothiazine (PTH) as a photoredox catayst under violet light irradiation, incorporating statistical copolymers and block copolymers into the existing nanonetwork. Hydrophilic and hydrophobic homo-and statistical copolymer incorporation leads to custom designed, tailored nanonetworks and stimuli-responsive behavior. For example, particles expanded by incorporation of PNIPAAM collapse after thermoresponsive behavior above 32 °C and shrink to approximately half of their original size. Furthermore, ABA triblocks and ABABA pentablocks of MA, TFEA, NIPAAM and tBA are integrated with a high degree of control into a parent particle. In this work, we have demonstrated the feasibility of parent nanonetwork structures to expand their network architecture reaching up to the microscale range to give soluble soft matter networks, containing controlled compositions of homopolymers, statistical copolymers, or pentablock structures. The taught concept gives opportunities to further design and alter the network topology in confined structures to tailor properties and function.

Received 1st May 2019, Accepted 24th June 2019 DOI: 10.1039/c9py00639g

rsc.li/polymers

Introduction

Amorphous polymer networks are one of the most fundamental materials in polymer science with applications that are governed by their complex dynamics, linear elasticity, network topology, and mechanical properties. It is accepted that heterogeneous crosslinking events occur during network formation creating imperfections that ultimately affect a network's connectivity and its resulting dynamics. Controlling crosslinking chemistry and allowing for the repair and restructuring of networks through integrated moieties is an increasing field of interest as it allows for control over a network's structure both during and after formation. Recently, postsynthetic modifications of polymer gels' chemical compositions and network properties have been achieved through

either the incorporation of atom transfer radical polymerization (ATRP) initiator sites within the parent gel network producing structurally tailored and engineered macromolecular (STEM) gels,^{17–20} or through the incorporation of trithiocarbonates (TTCs) in the parent network crosslinks²¹ which, with the advancement of photo-controlled radical polymerizations and new photocatalysts,^{22–24} resulted in the development of a living additive manufacturing method.²⁵ In each case properties of the parent gels were manipulated by growing secondary polymer chains into the existing network from the embedded initiators, producing daughter gels containing new properties provided by and dependent upon the newly introduced polymer chains.

In our recent communication, we adapted this concept to the expansion of nanonetwork materials, which in contrast to the above material is not a gel but rather a macromolecular network fully soluble in organic solvents. ²⁶ In a proof-of-concept study, the photocontrolled growth of nanonetworks was achieved through polymerizations from the integrated trithiocarbonate crosslinker by either direct photolysis or by photoredox catalysis. Integration of linear polymers into the nanonetwork yielded improved dispersities in contrast to the

^aUniversity of Houston, Department of Chemistry, Center for Excellence in Polymer Chemistry, Cullen Blvd., Houston, TX, 77004, USA. E-mail: harth@uh.edu

^bVanderbilt University, Department of Chemistry, Stevenson Center, Nashville, TN, 37235. USA

[†]Electronic supplementary information (ESI) available: Detailed experimental data and all spectroscopy data. See DOI: 10.1039/c9py00639g

parent nanonetworks and improved control over the polymerization was achieved by performing the polymerizations with 10-phenylphenothiazine (PTH) as a photocatalyst.²⁶ These results along with the successful reports of property manipulations in polymer gels encouraged us to further test the controlled modification of our nanonetwork system by altering the network composition, architecture, and properties.

Herein, we sought to investigate the controlled manipulation of photogrowable nanonetworks' (PGNNs) sizes and properties by utilizing a breadth of monomer families to form homopolymers with hydrophilic or hydrophobic character from acrylates, acrylamides and fluorinated monomers such as tert-butyl acrylate (tBA), trifluoroethyl acrylate (TFEA), hydroxyethyl acrylate (HEA), and stimuli responsive N-isopropyl acrylamide (NIPAAM). Control provided by this process allows for the preparation of other polymer compositions in the form of statistical copolymers containing methyl acrylate (MA) (PMA-co-PTFEA, PMA-co-PtBA, and PMA-co-PHEA) and block copolymers. The symmetrical nature of the trithiocarbonate is ideal to grow ABA triblock and ultimately ABABA pentablock copolymers through the addition of three monomers to form PMA-b-PTFEA-b-PMA-b-PTFEA-b-PMA, PMA-b-PtBA-b-PMA-b-PtBA-b-PMA, PMA-b-PNIPAAM-b-PMA-b-PNIPAAM-b-PMA, and PMA-b-PHEA-b-PMA pentablock copolymers. Utilizing this controlled photogrowth process we are able to tailor multiple progeny networks with altered network compositions, sizes, and properties stemming from a single parent network on the nanoscale.

Results and discussion

Crosslinked nanonetworks derived from our developed intermolecular chain crosslinking process with integrated trithio-carbonates²⁶ (PGNNs) are ideal candidates for photoredox mediated polymerizations with the aim to extend the network architecture through linear polymers, as the parent and resulting particles are soluble in organic solvents which allows for advantageous conditions during polymerization and characterization.²⁶ To further develop and investigate the scope of possible nanonetwork modifications, representative monomers such as *tert*-butyl acrylate (*tBA*), *trifluoroethyl* acrylate (TFEA), hydroxyethyl acrylate (HEA), *N*-isopropyl acrylamide (NIPAAM) and polymer compositions in the form of homopolymers, statistical copolymers, and ABA tri- and ABABA pentablock copolymers were integrated into the crosslinker of the network structure (Fig. 1).

Parent PGNNs were prepared as previously described; briefly a poly (methyl methacrylate-co-glycidol methacrylate) copolymer was synthesized through reversible addition-fragmentation chain transfer (RAFT) polymerization as one of the nanoparticle components with MW = 6200 g mol $^{-1}$, D=1.09 and 19% incorporation of glycidyl methacrylate (Scheme 1). The dithiobenzoate RAFT end group was removed by aminolysis and the resulting thiol capped with methyl methacrylate to ensure polymerization could only occur from the TTC cross-

linker. Pendant epoxides were ring opened with thioacetic acid followed by a triethylamine promoted sulfur to oxygen acetyl migration to provide a thiolated polymer (ESI). Parent PGNNs were then prepared through thiol maleimide click chemistry using the thiolated polymer at a concentration of 0.005 M with 2 equivalents (with respect to mmol of thiol) of the symmetrical bis-maleimide cross-linker26 with integrated trithiocarbonate producing nanonetworks with a size of 43 ± 10 nm by TEM and 66 ± 11 nm by DLS (Scheme 2). As the concentration of the active unit in the polymer and the equivalents of the crosslinking unit determines the size of the nanoparticle, we used a ratio that gives particles well below 100 nm for the investigation of the photogrowth process as a means to better illustrate the range of nanonetwork dimensions that can be achieved. Free maleimides on the nanonetwork surface were then reacted with furan in a Diels-Alder reaction to prevent the maleimides from interfering in future polymerizations. Although only an intermolecular crosslinking is desired during our network formation, intramolecular crosslinking is unavoidable and will result in the formation of loops. However, the number of loops present within a network and the behavior of loops during the photogrowth process is currently unknown.

Model polymerizations

A series of model photoredox polymerizations were performed with PTH as a photocatalyst and a thiol capped crosslinker 1a (Scheme S1†) to obtain optimized conditions to produce homopolymers, statistical copolymers, and block copolymers with the desired monomers. Model homopolymerizations revealed that a high level of control over dispersity ($D \le 1.14$) can be obtained for each monomer with the exception of HEA (D = 1.31) and that polymerizations in acetonitrile (MeCN) progress slower than in dimethyl sulfoxide (DMSO) (Fig. S1†) as demonstrated by the polymerization of MA. Additionally, homopolymers of TFEA produce a negative refractive index (RI) response in GPC with dimethyl formamide (DMF) as the eluent which is expected when fluorinated polymers have a smaller refractive index than the eluent.27-29 Model statistical copolymerizations produced good control over dispersity ($D \leq$ 1.17) for each copolymer pair (MA-tBA, MA-TFEA, MA-HEA) (Fig. S2†). As expected, the small incorporation of TFEA randomly in a copolymer with MA does not produce a negative RI response in GPC. Lastly, model polymerizations to produce ABA triblock and ABABA pentablock copolymers with MA (A) and another monomer (B) demonstrated excellent control over dispersity with tBA and TFEA ($D \le 1.14$), while block copolymers that incorporated HEA or NIPAAM displayed increased dispersity ($D \le 1.33$) (Fig. S3†). Interestingly, PMA-b-PTFEA-b-PMA triblock copolymers display both a weak negative and a weak positive RI response as opposed to the expected negative response. GPC analysis of molecular weight and dispersity of this polymer were not reported due to the disruption of the baseline and the presence of these overlapping responses. Further chain extension with MA to produce the PMA-b-PTFEA-b-PMA-b-PTFEA-b-PMA pentablock yields only a positive

Polymer Chemistry Paper

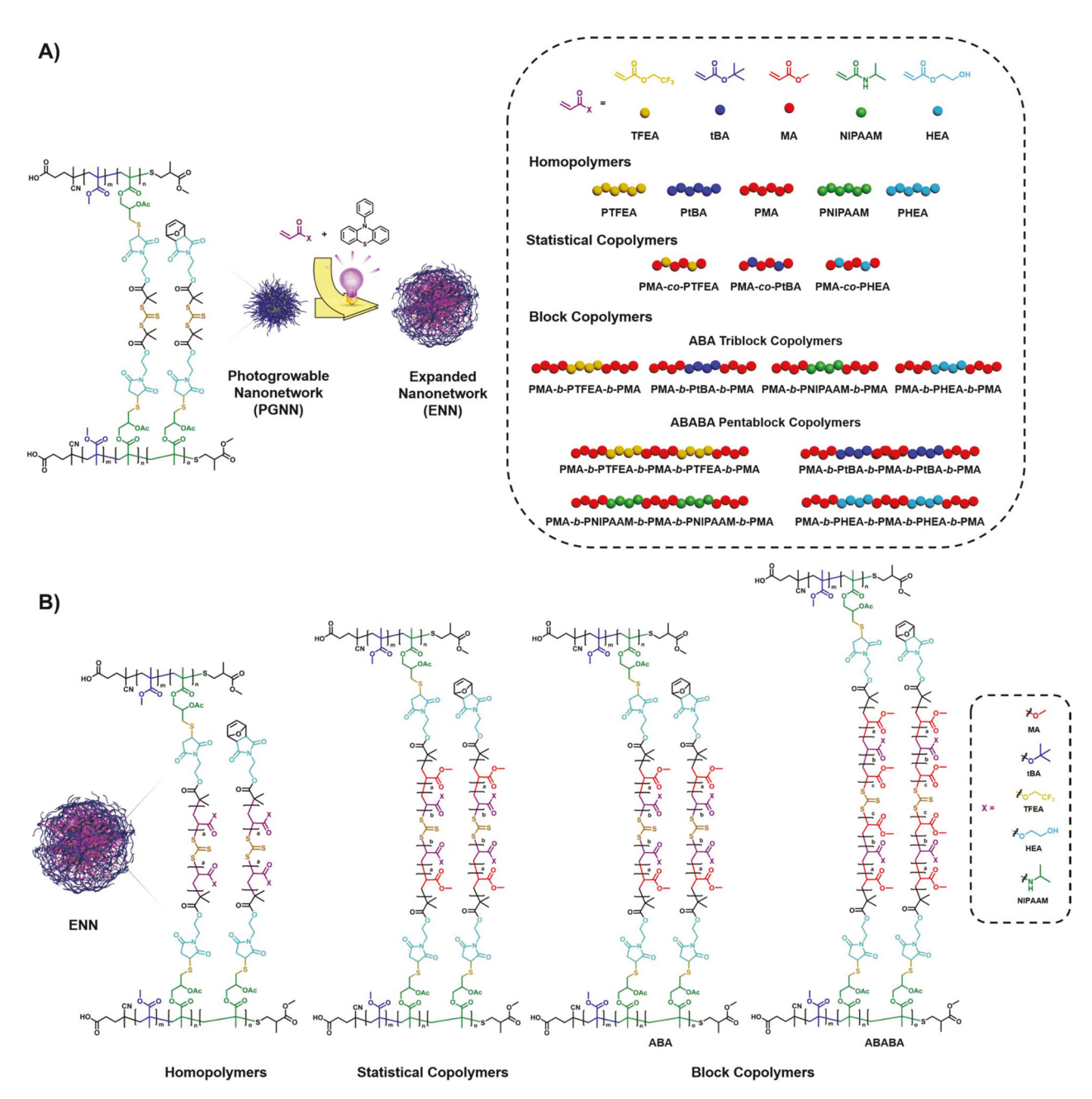
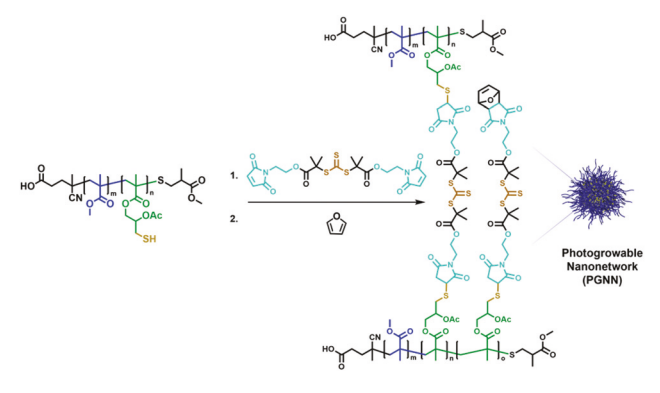


Fig. 1 (A) Structure and expansion of nanonetworks through the incorporation of various monomers, and the list of polymers that can be incorporated into the networks. (B) The general structure of expanded networks with incorporated homopolymers, statistical copolymers, and block copolymers.

Scheme 1 Synthesis of thiolated polymer.²⁶

Paper Polymer Chemistry



Scheme 2 Synthesis of photogrowable nanonetwork.²⁶

response. This reversion to a single positive peak can be explained by the increase in refractive index provided by the new PMA block.

Homopolymer incorporation

Next, optimized experimental conditions were applied to PGNNs to investigate the expansion of nanonetworks with various monomers (Fig. 2 and Table 1). Parent nanonetworks were exposed to the desired monomer (1 M) and solvent and were then irradiated for 30, 60 or 240 minutes in the presence of PTH. Expansion reactions were then purified by dialysis. Given that the parent PGNN and all the produced daughter ENNs are soluble in organics, nanonetworks were analysed by GPC and NMR to confirm the successful incorporation of new monomer units (ESI). While GPC analysis of these nanonetworks does not yield true reflections of their molecular weights, it does offer easily accessible evidence that a change has occurred within the network that is a direct result of the incorporation of new monomer units. GPC analysis of all homopolymer ENNs revealed a shift towards higher molecular weight and an increase in dispersity ($D \le 1.86$) when compared

to the parent PGNN (D = 1.53) (Fig. 2). The average change in dispersity across all monomers, after 30 minutes of irradiation, $(\Delta D_{\rm avg} \approx 0.22)$ agrees with our previous findings for MA homopolymerizations ($\Delta D_{\rm avg} \approx 0.18$).²⁶ Irradiation with the photocatalyst produced an increase in the diameter of the parent PGNN in the case of each monomer, with longer irradiation times producing larger daughter ENNs as confirmed by TEM and DLS measurements. Homopolymer expansion of PGNNs with tBA proceeded slower than other monomers investigated. This was attributed in part to the steric hinderance provided by the tert-butyl ester which may hinder the incorporation of additional monomers within the network structure (Table 1). Expansions with TFEA produced ENNs that displayed a negative RI response on GPC as expected from the model polymerization. This negative response is indicative that the RI of the nanonetwork has changed as a result of the formation of new polymer chains and points toward the possibility of being able to produce nanonetworks with tuneable RIs. Samples irradiated for 60 min, showed an increased molecular weight, size, and in most cases slight increases in dispersities were observed. In order to probe the limits of the expansion process, an expansion with MA was performed for 240 min which resulted in ENNs with sizes around 1000 nm. Irradiation times longer than 240 min yielded no further increase in network diameter.

Aminolysis of homopolymer ENNs

To gain a better understanding of the control over polymerizations within the nanonetworks, a promoted network disassembly was performed on each ENN. Promoted network disassembly proceeds through aminolysis of the crosslinker TTC with piperidine resulting in branched polymers (BPs) (Fig. 3A). Exposure of the parent **PGNN** to piperidine resulted in **BP** with $M_n = 7600 \text{ g mol}^{-1}$ and D = 1.14. GPC analysis of the promoted disassembly of each homopolymer ENN after 30 minutes reveals an increase in molecular weight in comparison to **BP**

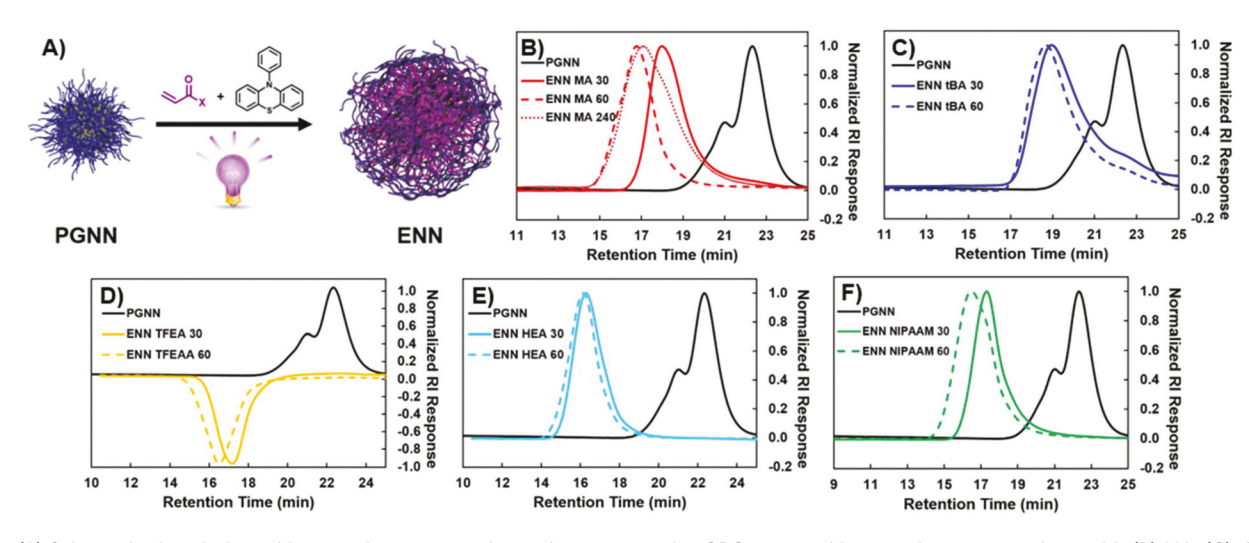


Fig. 2 (A) Schematic description of homopolymer expansions of nanonetworks. GPC traces of homopolymer expansions with (B) MA, (C) tBA, (D) TFEA, (E) HEA, and (F) NIPAAM at 30 and 60 minutes irradiation times.

Table 1 Homopolymer expansions of PGNNs

#	Sample	Monomer	Irradiation time (min)	PTH (mol%)	Solvent	$M_{\text{n GPC}}^{a}$ (g mol ⁻¹)	D^a	Diameter _{TEM} (nm)	Diameter _{DLS} (nm)
1	PGNN	_	0	_	_	9800	1.53	43 ± 10	66 ± 11
2	ENN MA 30	MA	30	0.02	DMSO	47 200	1.79	250 ± 60	290 ± 95
3	ENN MA 60	MA	60	0.02	DMSO	132 000	1.84	584 ± 146	612 ± 165
4	ENN MA 240	MA	240	0.10	MeCN	81 400	2.10	1022 ± 327	1354 ± 567
5	ENN tBA 30	tBA	30	0.10	MeCN	21 000	1.60	182 ± 56	231 ± 118
6	ENN tBA 60	tBA	60	0.10	MeCN	25 900	1.63	225 ± 70	263 ± 115
7	ENN TFEA 30	TFEA	30	0.02	MeCN	102 000	1.42	266 ± 47	300 ± 71
8	ENN TFEA 60	TFEA	60	0.02	MeCN	153 000	1.80	361 ± 85	395 ± 101
9	ENN HEA 30	HEA	30	0.02	DMSO	173 000	1.74	162 ± 78	193 ± 84
10	ENN HEA 60	HEA	60	0.02	DMSO	226000	1.87	241 ± 90	283 ± 130
11	ENN NIPAAM 30	NIPAAM	30	0.005	MeCN	62 000	1.86	197 ± 75	250 ± 65
12	ENN NIPAAM 60	NIPAAM	60	0.005	MeCN	119000	2.31	319 ± 95	372 ± 90

^a Molecular weight and polydispersity were determined by GPC analysis with DMF as eluent at 1 ml min⁻¹ at 60 °C.

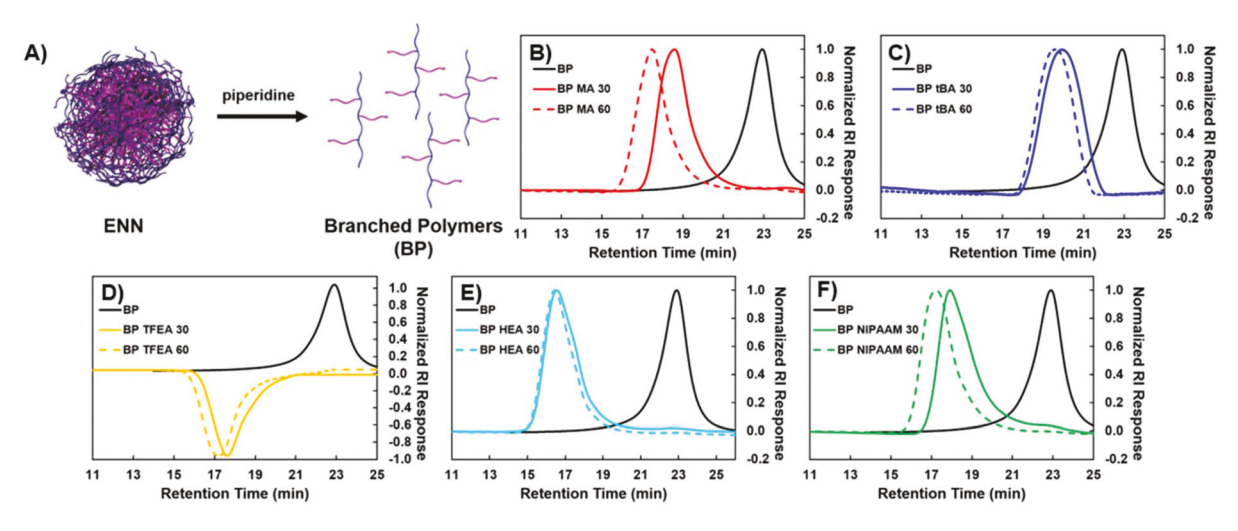


Fig. 3 (A) Schematic description of the selective cleavage of nanonetworks to produce branched polymers. GPC traces of the resulting branched polymers from homopolymer expansions of (B) MA, (C) tBA, (D) TFEA, (E) HEA, and (F) NIPAAM.

for each monomer. Dispersity of these BPs remains relatively low ($D \leq 1.42$) for each of the investigated monomers except for HEA which displayed a higher dispersity of 1.60. In all cases BPs produced after 60 minutes of irradiation show an increase in molecular weight when compared to those produced at 30 minutes. BPs produced from tBA, TFEA, and HEA after 60 minutes display a narrowing of dispersity from 30 minutes, while MA and NIPAAM display a slight increase at this extended reaction time (Fig. 3 and Table 2). Although all BPs displayed a higher dispersity when compared to the parent BP, it should be noted that the difference in dispersity from 30 to 60 minutes is small ($\Delta D < 0.1$) in all cases except for NIPAAM, the dispersity decreases from 30 to 60 minutes in the majority of cases, and in all cases the dispersity remains relatively low ($D \leq 1.60$).

Thermoresponsive behavior of PNIPAAM ENNs

Encouraged by the successful incorporation of these monomer families, we sought to explore the properties that can arise as a result from the altered chemical composition of these daugh-

Table 2 Aminolysis of homopolymer nanonetwork expansions

#	Sample	$M_{\text{n GPC}}^{a} (\text{g mol}^{-1})$	D^a
1	BP	7600	1.14
2	BP MA 30	31 900	1.30
3	BP MA 60	112 000	1.38
4	BP tBA 30	19 000	1.22
5	BP tBA 60	23 300	1.21
6	BP TFEA 30	85 000	1.42
7	BP TFEA 60	136 500	1.37
8	BP HEA 30	168 000	1.60
9	BP HEA 60	209 000	1.55
10	BP NIPAAM 30	58 000	1.37
11	BP NIPAAM 60	106 000	1.55

 $[^]a$ Molecular weight and polydispersity were determined by GPC analysis (DMF as eluent).

ter nanonetworks. For example, we evidenced a change of the tailorable nanonetwork RI through the polymerization of TFEA, and we explored the effects that the introduction of HEA would have on nanonetwork solubility. Parent PGNNs are in-

Paper

soluble in water; however, by incorporating PHEA chains within the nanonetwork a fully water soluble ENN can be produced. Likewise, water soluble nanonetworks can be prepared through the incorporation of PNIPAAM chains within the nanonetwork.

Armed with the knowledge that PNIPAAM ENNs are water soluble we aimed to investigate if these daughter networks inherited the thermoresponsive behaviour of PNIPAAM. It is well known that PNIPAAM has a lower critical solution temperature (LCST) at 32 °C in water above which PNIPAAM expunges water and experiences a chain collapse resulting in a shrunken polymer.30 We reasoned that if a daughter network expanded with PNIPAAM possessed these thermoresponsive properties then it could be feasible to induce a chain collapse that results in the shrinkage of PNIPAAM polymers and ultimately the ENN itself by merely heating the ENN above 32 °C. To probe this, we designed an experiment in which PNIPAAM ENNs after 30 (ENN NIPAAM 30) and 60 (ENN NIPAAM 60) minute irradiation times were dissolved in water and the diameter measured by DLS every two degrees over a temperature range of 25 °C-45 °C. The average size of each ENN was first determined in water at 25 °C resulting in an average size of ~239 nm for ENN NIPAAM 30 and ~383 nm for ENN NIPAAM 60. Upon heating above 32 °C we observe a sharp decrease in diameter for ENN NIPAAM 30 to ~70 nm and a more gradual decrease for ENN NIPAAM 60 to ~200 nm (Fig. 4). Additional heating to 45 °C provided no changes nanonetwork diameters. To ensure that the observed change in diameter was due to the formation of PNIPAAM chains and was independent of the properties of the parent nanonetwork, a control experiment was performed. Because, the parent PGNN is insoluble in

water, but HEA ENNs are water soluble and should not possess thermoresponsive properties, the HEA ENNs (ENN HEA 60) were used as control networks. The average size of ENN HEA 60 was found to be ~560 nm, and heating through 32 °C to 45 °C produced no meaningful change in diameter. Thus, we can conclude that the change in diameter at 32 °C is indeed caused by the incorporation of PNIPAAM. To further illustrate the thermoresponsive behaviour of PNIPAAM ENNs, images displaying the nanonetworks fully dissolved in water at 25 °C are compared to images of nanonetworks after being heated above the LCST (40 °C) (Fig. 4). It is clear that HEA ENNs are unaffected by the change in temperature, while the NIPAAM ENNs display increased turbidity as a result of the increase in temperature, with the change in turbidity being more apparent with larger nanonetworks. The success of these experiments is encouraging as it demonstrates the potential to produce highly tailorable and stimuli responsive nanomaterials.

Incorporation of statistical copolymers

After having successfully demonstrated the addition of each monomer into the parent PGNN, we aimed to explore the introduction of polymer compositions in the form of statistical copolymers or block copolymers from these investigated monomer families. First, we examined the incorporation of copolymers from MA/tBA, MA/TFEA, and MA/HEA with MA being the major monomer component. MA was chosen as the major component in each composition due to its flexibility to be polymerized in either MeCN or DMSO and still provide good control over dispersity. Copolymer ENNs were prepared by first exposing the parent PGNN to a 1 M solution of MA and the desired comonomer in an 80/20 ratio respectively with the

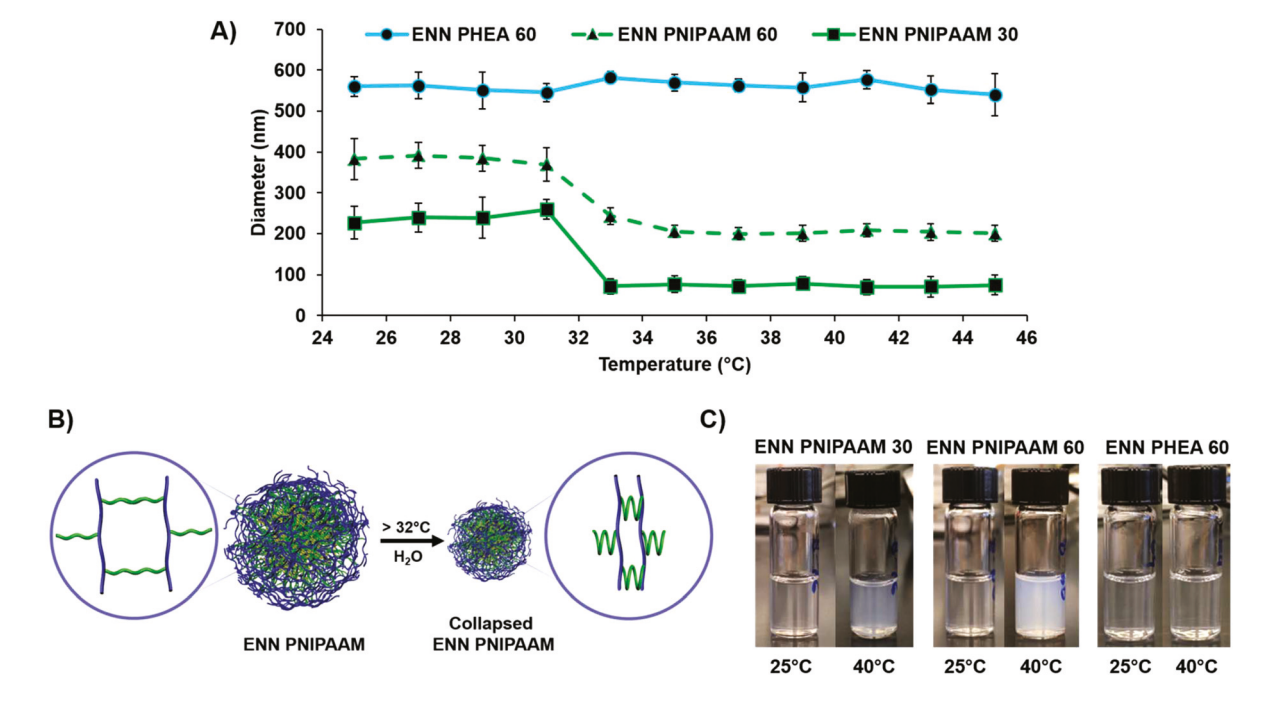


Fig. 4 (A) DLS diameter measurements of NIPAAM and HEA ENNs across 25–45 °C. (B) Schematic description of PNIPAAM chain collapse above 32 °C producing shrunken nanonetworks. (C) Images of solutions of NIPAAM and HEA ENNs at 25 °C and 40 °C.

Polymer Chemistry Paper

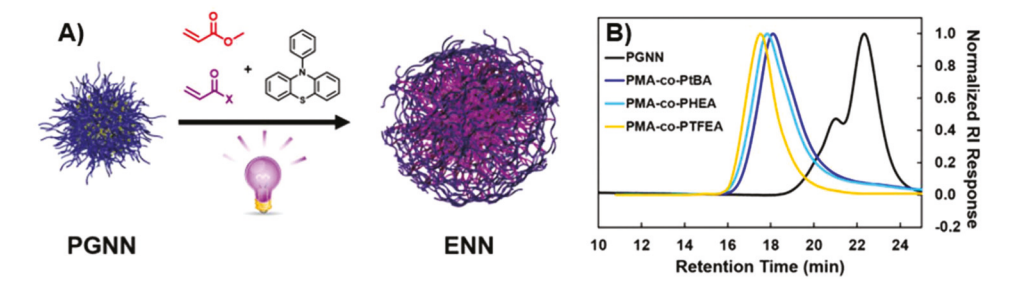


Fig. 5 (A) Schematic description and (B) GPC traces of statistical copolymer expansions of nanonetworks.

appropriate solvent. Nanonetworks were then irradiated in the presence of PTH for 30 minutes and then purified by dialysis. Analysis of the produced copolymer ENN by GPC reveals a shift toward higher molecular weight and a slight increase in dispersity in each case (Fig. 5). Interestingly, the dispersity observed for copolymer ENNs with MA ($D \le 1.59$) is less than the dispersity observed for homopolymer ENNs of MA (D =1.79). Analysis by TEM and DLS showed an increase in the diameter from the parent PGNN with sizes similar to those produced from MA homopolymer ENNs (Table 3). NMR analysis displayed incorporations of tBA and HEA to be elevated compared to those observed in the model copolymerizations, while incorporations of TFEA closely matched those of the model (Table S2†). These successful copolymerizations demonstrate the potential to incorporate controllable quantities of a desired functional group which can facilitate further chemical modifications.

Incorporation of ABA tri- and ABABA pentablock copolymers

Next, we examined the possibility of producing ABA triblock and ABABA pentablock copolymers as the incorporation of block copolymer structures into these nanonetworks could produce particles that exhibit microphase separation behavior providing an interesting opportunity to examine the effects this would have on a pre-existing nanonetwork. Given ENNs still have the integrated TTCs after expansion, ENNs can be used as macroinitiators to produce further expanded nanonetworks rendering them capable of producing block copolymers. For the production of ABA and ABABA block copolymers MA was chosen as the "A" block for both its solvent and monomer compatibility and the desired monomer as the "B" block. Pentablock ENNs were prepared by first preparing a MA

homopolymer ENN (ENN 1) as previously described. ENN 1 was then used to prepare ABA triblock copolymers with each monomer (tBA, TFEA, HEA, NIIPAAM) by exposing ENN 1 to the appropriate conditions determined in the model block copolymerizations. Further expansion from ENN 1 with each monomer results in four ABA triblock copolymers: PMA-b-PtBA-b-PMA (ENN 2), PMA-b-PHEA-b-PMA (ENN3), PMA-b-PNIPAAM-b-PMA (ENN 4), and PMA-b-PTFEA-b-PMA (ENN 5). Utilizing the triblock ENNs as macroinitiators, ABABA pentablock ENNs can be prepared by performing chain extensions with MA. Chain extensions from each tri block results in four pentablock copolymer ENNs: PMA-b-PtBA-b-PMA-b-PtBA-b-PMA (ENN 6), PMA-b-PHEA-b-PMA-b-PMA-b-PMA-b-PMA (ENN 7), PMA-b-PNIPAAM-b-PMA-b-PMA-b-PMA (ENN 8), and PMA-b-PTFEA-b-PMA-b-PTFEA-b-PMA (ENN 9).

Analysis of ENN 1 reveals the expected increase in diameter, molecular weight, and dispersity that was observed in the previous homopolymerizations. GPC analysis of ABA triblocks displays a shift towards higher molecular weight and increased dispersity (Fig. 6). Both HEA and NIPAAM triblocks experience slight increases in dispersity (D = 1.81) compared to ENN 1 (D = 1.72) (Table 4). **ENN** 5 produces the same weak negative and weak positive RI response in GPC that were observed in the model block copolymerizations with TFEA and so molecular weight and dispersity were not reported for this nanonetwork. ENN 2, prepared from tBA, experiences a more pronounced increase in dispersity (D = 2.38) than the other ENNs when compared to ENN 1 (D = 1.72). Closer examination of the GPC trace reveals low molecular weight tailing which is attributed to only partial polymerization participation of ENN 1 with tBA. Size characterization by TEM and DLS showed an increase in diameter with each triblock ENN when compared to ENN 1.

Table 3 Statistical copolymer expansions of PGNNs

#	Sample	Monomers (MA/X)	Irradiation time (min)	Solvent	$M_{\text{n GPC}}^{a}$ (g mol ⁻¹)	D^a	Monomer incorporation b (MA/X)	Diameter _{TEM} (nm)	Diameter _{DLS} (nm)
1	PGNN	_	0	_	9800	1.53	_	43 ± 10	66 ± 11
2	PMA-co-PtBA	MA/tBA (80/20)	30	MeCN	26 000	1.58	67/33	220 ± 112	283 ± 130
3	PMA-co-PHEA	MA/HEA (80/20)	30	DMSO	63 700	1.58	69/31	381 ± 103	420 ± 135
4	PMA-co-PTFEA	MA/TFEA (80/20)	30	DMSO	87 000	1.59	74/26	302 ± 100	332 ± 140

Reactions were performed with 0.02 mol% PTH. ^a Molecular weight and polydispersity were determined by GPC analysis (DMF as eluent). ^b Monomer incorporation was determined by ¹H NMR.

Paper

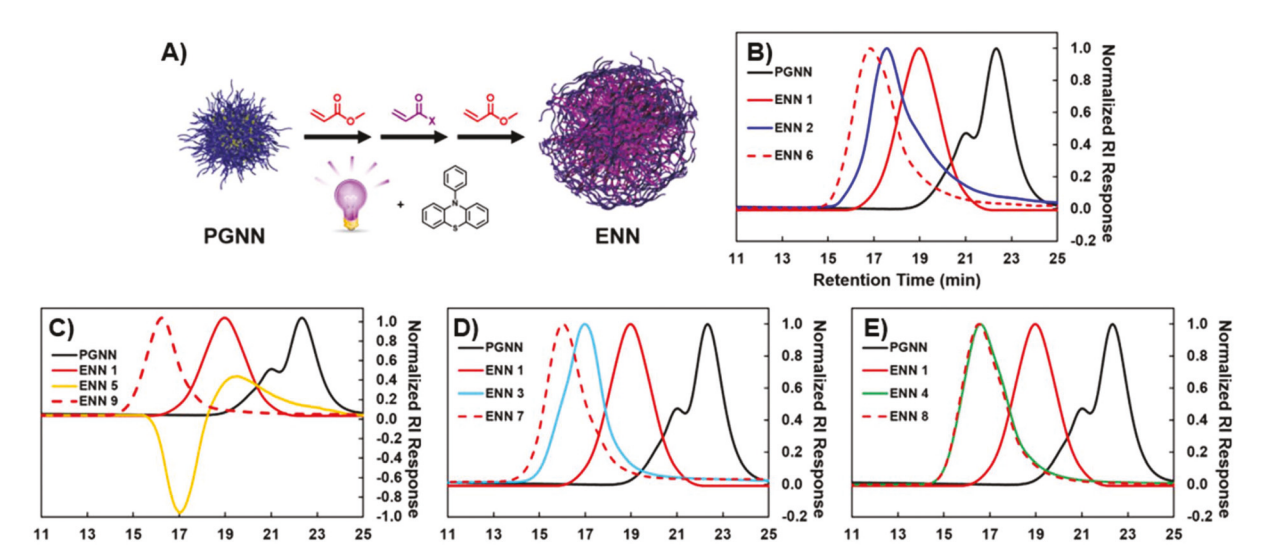


Fig. 6 (A) Schematic description of ABA block copolymer expansion of nanonetworks. GPC traces of block copolymer expansions with (B) tBA, (C) HEA, (D) TFEA, and (E) NIPAAM.

Table 4 Block copolymer expansions of PGNNs

#	Sample	Macro- initiator (MI)	$\begin{array}{c} \operatorname{MI} M_{\mathrm{n, GPC}}^{a} \\ \left(\operatorname{g mol}^{-1} \right) \end{array}$	$\mathbf{MI} \ \boldsymbol{\mathit{D}}^{a}$	Monomer	$M_{\text{n GPC}}^{a}$ (g mol ⁻¹)	D^a	$\begin{array}{c} Diameter_{TEM} \\ (nm) \end{array}$	Diameter _{DLS} (nm)
1	PGNN	_	9800	1.53	_	9800	1.53	43 ± 10	66 ± 11
2	ENN 1 (PMA)	PGNN	9800	1.53	MA	30 000	1.72	273 ± 60	302 ± 98
$3^{b,c}$	ENN 2 (PMA-b-PtBA-b-PMA)	ENN 1	30 000	1.72	tBA	50 500	2.38	325 ± 131	355 ± 157
4	ENN 3 (PMA-b-PHEA-b-PMA)	ENN 1	30 000	1.72	HEA	118 000	1.81	347 ± 86	387 ± 92
$5^{b,d}$	ENN 4 (PMA-b-PNIPAAM-b-PMA)	ENN 1	30 000	1.72	NIPAAM	149000	1.81	375 ± 77	413 ± 97
6^b	ENN 5 (PMA-b-PTFEA-b-PMA)	ENN 1	30 000	1.72	TFEA	_	_	482 ± 55	518 ± 98
$7^{b,c}$	ENN 6 (PMA-b-PtBA-b-PMA-b-PtBA-b-PMA)	ENN 2	50 500	2.38	MA	119 000	1.98	420 ± 103	482 ± 144
8	ENN 7 (PMA-b-PHEA-b-PMA-b-PHEA-b-PMA)	ENN 3	118 000	1.81	MA	289 000	1.96	452 ± 122	493 ± 145
9	ENN 8 (PMA-b-PNIPAAM-b-PMA-b-PNIPAAM-b-PMA)	ENN 4	149 000	1.81	MA	175 000	1.87	402 ± 115	438 ± 167
10	ENN 9 (PMA-b-PTFEA-b-PMA-b-PTFEA-b-PMA)	ENN 5	_	_	MA	272 000	1.74	613 ± 151	651 ± 183

Reactions were performed in DMSO with 0.02 mol% PTH unless otherwise indicated. ^a Molecular weight and polydispersity were determined by GPC analysis (DMF as eluent). ^b Reactions were performed in MeCN. ^c Reactions were performed with 0.1 mol% PTH. ^d Reactions were performed with 0.005 mol% PTH.

Characterization of triblocks by ¹H NMR confirmed the successful production of new polymer chains through the appearance of peaks unique to the desired monomers such as the *tert*-butyl, isopropyl, fluorinated ester, and hydroxy ethyl ester moieties (Fig. S18–S21†).

As expected, GPC analysis of ABABA pentablock ENNs shows a shift towards higher molecular weight and in the case of HEA and NIPAAM a slight increase in dispersity. Interestingly, ENN 6, experienced a narrowing of dispersity to D=1.98 from its macroinitiator's, ENN 2, dispersity of 2.38. Accompanying this narrowing was a reduction in the lower molecular weight tailing that was previously observed. This suggests that the nanonetworks that comprised the tailing were still capable of mediating radical polymerizations and thus capable of experiencing the photocontrolled growth process. As demonstrated in the model block copolymerizations, ENN 9 experiences a reversion to a positive RI response in GPC from ENN 5 as a result of the new PMA block.

Remarkably, the dispersity of all pentablock ENNs remained lower than 2.0, which is a strong indication of the fidelity and control of the photoredox mediated polymerizations. Further characterization of pentablock ENNs by ¹H NMR confirms the installation of a new PMA block within the nanonetwork as we can observe a clear increase in the intensity of the methyl ester peak in each pentablock ENN.

Aminolysis of ABA tri- and ABABA pentablock ENNs

Once again, we implemented a promoted disassembly to gain a clearer understanding of the control obtained during the expansion process of ABA and ABABA block copolymer ENNs (Fig. 7). Aminolysis products of the PMA ENN macroinitiator (**BP 1**) displayed an increase of 20 000 g mol⁻¹ and D = 1.24 compared to the parent PGNN (**BP**) with $M_{\rm n} = 7600$ g mol⁻¹ and D = 1.14 (Table 5). Disassembly products of the triblock ENNs exhibited increases in molecular weight as well as increases in dispersity with D < 1.70. Aminolysis of the PMA-b-

Polymer Chemistry

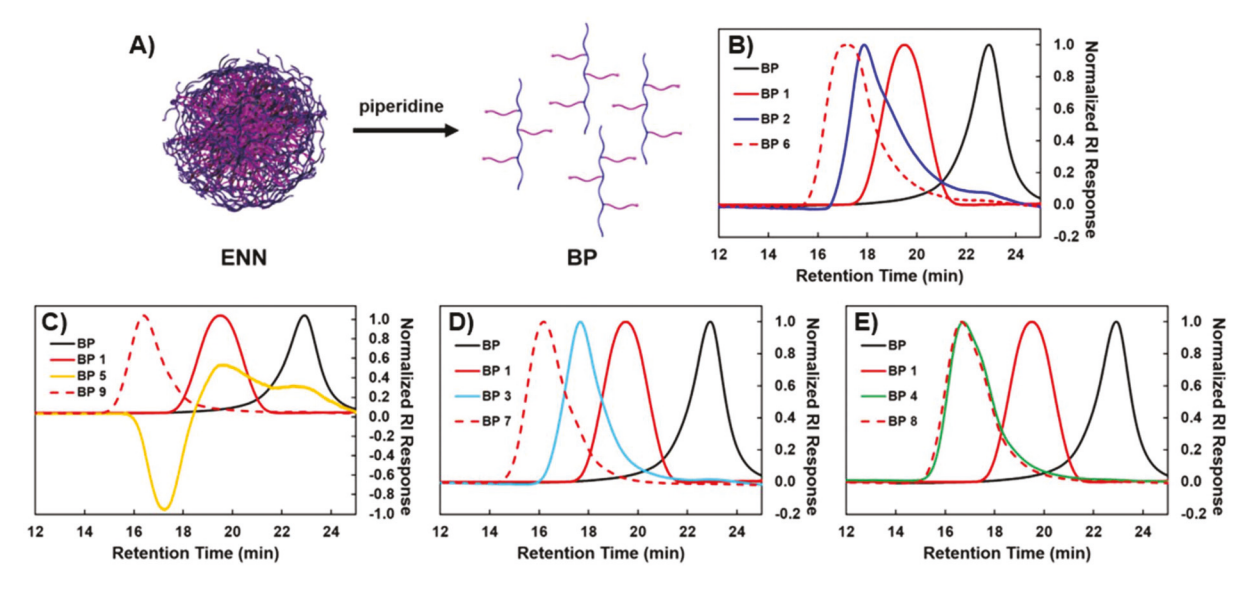


Fig. 7 (A) Schematic description of the selective cleavage of nanonetworks to produce branched polymers. GPC traces of the resulting block copolymer expansions with (B) tBA, (C) HEA, (D) NIPAAM, and (E) TFEA.

Table 5 Aminolysis of block copolymer nanonetwork expansions

#	$sample^a$	$M_{\mathrm{n~GPC}}^{b}\left(\mathrm{g~mol^{-1}}\right)$	D^b
1	BP	7600	1.14
2	BP 1 (PMA)	27 000	1.24
3	BP 2 (PMA- b -P t BA)	56 000	1.48
4	BP 3 (PMA-b-PHEA)	100 000	1.67
5	BP 4 (PMA-b-PNIPAAM)	132 000	1.69
6	BP 5 (PMA-b-PTFEA)	_	_
7	BP 6 (PMA- <i>b</i> -PtBA- <i>b</i> -PMA)	103 000	1.69
8	BP 7 (PMA-b-PHEA-b-PMA)	231 000	1.79
9	BP 8 (PMA-b-PNIPAAM-b-PMA)	139 000	1.79
10	BP 9 (PMA-b-PTFEA-b-PMA)	265 000	1.34

^a Branched block copolymers as they appear once cleaved from either the tri- or pentablock copolymer ENNs. b Molecular weight and polydispersity were determined by GPC analysis (DMF as eluent).

PTFEA-b-PMA triblock produces a PMA-b-PTFEA diblock copolymer which exhibits a similar positive and negative RI response in GPC therefore analysis of molecular weight and dispersity were not reported. Promoted disassembly of ABABA pentablock ENNs once again revealed an increase in both molecular weight and dispersity for blocks with tBA, NIPAAM, and HEA with D < 1.8. Interestingly, **BP 9** of the pentablock ENN containing TFEA possessed a relatively low dispersity of D = 1.34.

Conclusions

A developed photoexpansion process opens the possibility to significantly alter the chemical topology of a unique nanonetwork by integrating linear polymer chains with various compositions (homopolymers, statistical copolymers, block copolymer) from a range of monomer families. Through this photoexpansion process a single parent nanonetwork can produce

multiple differentiated progeny that inherit properties of the newly incorporated polymers which allows for the manipulation of RI, the transformation of water-insoluble parent particles into water soluble structures, and the transformation of thermally unresponsive parent networks into thermally responsive daughter networks. Furthermore, the integration of ABA and ABABA block copolymers, with their known microphase separation behavior, can prove beneficial to produce model systems to examine effects of introducing block copolymer architectures into an existing nanonetwork on network topology and organization. The ability to control and integrate a variety of linear homopolymers, copolymers, or block copolymers into parent nanonetworks will allow for targeted manipulations of the chemical structure and physical properties to facilitate investigations of network topologies.

Conflicts of interest

There are no conflicts to declare.

Acknowledgements

E. H. and M. W. L. are grateful for support from the Robert A. Welch Foundation through the Center of Excellence in Polymer Chemistry (Grant #H-E-0041) and funding from the National Science Foundation with the Award #1808664 (CHEM). The authors would also like to thank the Professor T. Randall Lee group for assistance and access to the Malvern Zetasizer Nanosystem (Defense University Research Instrumentation program grant (FA9550-15-1-0374) issued by the Air Force Office of Scientific Research).

Paper

Notes and references

- 1 T.-S. Lin, R. Wang, J. A. Johnson and B. D. Olsen, *Macromolecules*, 2019, 52, 1685–1694.
- 2 Y. Gu, J. Zhao and J. A. Johnson, *Trends Chem.*, 2019, 1(3), 318–334.
- 3 R. Wang, A. Alexander-Katz, J. A. Johnson and B. D. Olsen, Phys. Rev. Lett., 2016, 116, 188302.
- 4 S. Seiffert and J. Sprakel, *Chem. Soc. Rev.*, 2012, 41, 909–930.
- 5 H. Aoki, S. Tanaka, S. Ito and M. Yamamoto, *Macromolecules*, 2000, 33, 9650–9656.
- 6 H. Zhou, J. Woo, A. M. Cok, M. Wang, B. D. Olsen and J. A. Johnson, *Proc. Natl. Acad. Sci. U. S. A.*, 2012, **109**, 19119–19124.
- 7 T.-S. Lin, R. Wang, J. A. Johnson and B. D. Olsen, *Macromolecules*, 2018, 51, 1224–1231.
- 8 F. Di Lorenzo and S. Seiffert, *Polym. Chem.*, 2015, **6**, 5515–5528.
- 9 J. Wang, T.-S. Lin, Y. Gu, R. Wang, B. D. Olsen and J. A. Johnson, ACS Macro Lett., 2018, 7, 244–249.
- 10 R. Wang, T.-S. Lin, J. A. Johnson and B. D. Olsen, ACS Macro Lett., 2017, 6, 1414–1419.
- 11 M. B. Gordon, J. M. French, N. J. Wagner and C. J. Kloxin, *Adv. Mater.*, 2015, 27, 8007–8010.
- 12 Y. Amamoto, H. Otsuka, A. Takahara and K. Matyjaszewski, *ACS Macro Lett.*, 2012, 1, 478–481.
- 13 Y. Amamoto, H. Otsuka, A. Takahara and K. Matyjaszewski, *Adv. Mater.*, 2012, **24**, 3975–3980.
- 14 Y. Amamoto, J. Kamada, H. Otsuka, A. Takahara and K. Matyjaszewski, Angew. Chem., Int. Ed., 2011, 50, 1660– 1663.
- 15 R. Nicolaÿ, J. Kamada, A. Van Wassen and K. Matyjaszewski, *Macromolecules*, 2010, 43, 4355–4361.
- 16 C. J. Kloxin, T. F. Scott, B. J. Adzima and C. N. Bowman, *Macromolecules*, 2010, 43, 2643–2653.

- 17 A. Beziau, A. Fortney, L. Fu, C. Nishiura, H. Wang, J. Cuthbert, E. Gottlieb, A. C. Balazs, T. Kowalewski and K. Matyjaszewski, *Polymer*, 2017, 126, 224–230.
- 18 J. Cuthbert, A. Beziau, E. Gottlieb, L. Fu, R. Yuan, A. C. Balazs, T. Kowalewski and K. Matyjaszewski, *Macromolecules*, 2018, 51, 3808–3817.
- 19 J. Cuthbert, T. Zhang, S. Biswas, M. Olszewski, S. Shanmugam, T. Fu, E. Gottlieb, T. Kowalewski, A. C. Balazs and K. Matyjaszewski, *Macromolecules*, 2018, 51, 9184–9191.
- 20 J. Cuthbert, M. R. Martinez, M. Sun, J. Flum, L. Li, M. Olszewski, Z. Wang, T. Kowalewski and K. Matyjaszewski, *Macromol. Rapid Commun.*, 2019, 1800876.
- 21 H. Zhou and J. A. Johnson, Angew. Chem., Int. Ed., 2013, 52, 2235–2238.
- 22 M. Chen, M. J. MacLeod and J. A. Johnson, *ACS Macro Lett.*, 2015, **4**, 566–569.
- F. A. Leibfarth, K. M. Mattson, B. P. Fors, H. A. Collins and
 C. J. Hawker, *Angew. Chem., Int. Ed.*, 2013, 52, 199–210.
- 24 J. T. Trotta and B. P. Fors, Synlett, 2016, 702-713.
- 25 M. Chen, Y. Gu, A. Singh, M. Zhong, A. M. Jordan, S. Biswas, L. T. J. Korley, A. C. Balazs and J. A. Johnson, ACS Cent. Sci., 2017, 3, 124–134.
- 26 M. W. Lampley and E. Harth, ACS Macro Lett., 2018, 7, 745–750.
- 27 E. H. Discekici, A. Anastasaki, R. Kaminker, J. Willenbacher, N. P. Truong, C. Fleischmann, B. Oschmann, D. J. Lunn, J. Read de Alaniz, T. P. Davis, C. M. Bates and C. J. Hawker, *J. Am. Chem. Soc.*, 2017, 139, 5939–5945.
- 28 H. Gong, Y. Zhao, X. Shen, J. Lin and M. Chen, *Angew. Chem., Int. Ed.*, 2018, 57, 333–337.
- 29 Q. Quan, H. Gong and M. Chen, *Polym. Chem.*, 2018, 9, 4161–4171.
- 30 H. G. Schild, Prog. Polym. Sci., 1992, 17, 163-249.